



Morphometry of human insular cortex and insular volume reduction in Williams syndrome

Jeremy D. Cohen^{a,f,*}, Jeffrey R. Mock^{a,h}, Taylor Nichols^f, Janet Zadina^a, David M. Corey^b, Lisa Lemen^{c,d}, Ursula Bellugi^e, Albert Galaburda^g, Allan Reiss^f, Anne L. Foundas^{a,d,h}

^a Neuroscience Program, Tulane University, New Orleans, LA, United States

^b Department of Psychology, Tulane University, New Orleans, LA, United States

^c Department of Curriculum and Instruction, Louisiana State University Health Sciences Center, New Orleans, LA, United States

^d Department of Radiology, Veterans Affairs Medical Center, New Orleans, LA, United States

^e Salk Institute Laboratory for Cognitive Neuroscience, La Jolla, CA, United States

^f Center for Interdisciplinary Brain Sciences Research, Stanford University School of Medicine, United States

^g Department of Neurology, Beth Israel Deaconess Medical Center, Harvard Medical School, Boston, MA, United States

^h Department of Neurology, Louisiana State University Health Sciences Center, New Orleans, LA, United States

ARTICLE INFO

Article history:

Received 4 April 2009

Received in revised form 29 June 2009

Accepted 1 July 2009

Keywords:

Insula

Morphometry

Native-space

Cortex

Williams syndrome

ABSTRACT

Functional imaging in humans and anatomical data in monkeys have implicated the insula as a multi-modal sensory integrative brain region. The topography of insular connections is organized by its cytoarchitectonic regions. Previous attempts to measure the insula have utilized either indirect or automated methods. This study was designed to develop a reliable method for obtaining volumetric magnetic resonance imaging (MRI) measurements of the human insular cortex, and to validate that method by examining the anatomy of insular cortex in adults with Williams syndrome (WS) and healthy age-matched controls. Statistical reliability was obtained among three raters for this method, supporting its reproducibility not only across raters, but within different software packages. The procedure described here utilizes native-space morphometry as well as a method for dividing the insula into connectivity-based sub-regions estimated from cytoarchitectonics. Reliability was calculated in both ANALYZE ($N = 3$) and BrainImageJava ($N = 10$) where brain scans were measured once in each hemisphere by each rater. This highly reliable method revealed total, anterior, and posterior insular volume reduction bilaterally (all p 's $< .002$) in WS, after accounting for reduced total brain volumes in these participants. Although speculative, the reduced insular volumes in WS may represent a neural risk for the development of hyperaffiliative social behavior with increased specific phobias, and implicate the insula as a critical limbic integrative region. Native-space quantification of the insula may be valuable in the study of neurodevelopmental or neuropsychiatric disorders related to anxiety and social behavior.

© 2009 Elsevier Ltd. All rights reserved.

1. Introduction

A variety of methods have been described for assessing insular morphometry, each of which has inherent, specific limitations. Previous attempts to measure the insula using an indirect method of measuring the cerebrospinal fluid (CSF) space in the Sylvian fossa (Foundas et al., 1996, 1997) revealed inferred reductions in insular volume in Alzheimer's disease. Insular volume reductions were inferred because the measurements were of CSF space in the Sylvian fossa, and increased CSF was assumed to equate to reduced insular cortex. Subsequently, this method yields no direct quantification of

insular volumes. Efficiency is the main advantage of semi-automated methods, such as voxel-based morphometry (VBM) or FreeSurfer (Desikan et al., 2006). While VBM has been used to show changes in insular morphometry (Karas et al., 2003, 2004), individuals with a clinical or developmental disorder may have variations in anatomical landmarks, such as gyrification, that are critical for normalization algorithms and automated measurements (Thompson et al., 2000a,b). Voxel-based morphometry is also a whole-brain statistical approach (Mechelli et al., 2005), and the current study was focused specifically on insular morphometry. FreeSurfer has difficulty correctly identifying the insula due to its complex boundaries, and does not label this region. It should be noted that the anatomical boundaries, gyri and sulci are visible in post-mortem brains and can be visualized on magnetic resonance imaging (MRI) scans (Naidich et al., 2004). One previous study that measured insula volume directly using volumetric MRI methodology

* Corresponding author. Address: Stanford School of Medicine, Department of Psychiatry and Behavioral Sciences, 401 Quarry Rd., MC 5795, Stanford, CA 94305, United States. Tel.: +1 (650) 498 4538; fax: +1 (650) 724 4794.

E-mail address: jcohen2@stanford.edu (J.D. Cohen).

(Crespo-Facorro et al., 2000), but this research group designed their own software package to measure the insula which runs only on a Linux platform. Therefore, a novel method was developed and used in the reported study. This method is similar in approach to the Crespo-Facorro method in its use of insular boundaries and native-space (i.e. non-warped, ACPC-aligned) morphometry. It differs from previous methods by including a procedure to attempt to estimate the two main insular sub-regions based on connectivity (Mesulam and Mufson, 1982a,b,c) and is not restricted to any particular software package. The insula is a multifunctional region of cortex, but its connectivity with other brain regions is topographically organized (Mesulam and Mufson, 1982a,b,c; Augustine, 1985, 1996; Craig, 2003; Dronkers, 1996; Oppenheimer et al., 1992; Yaxley et al., 1990). While the current method is based primarily on anatomical data from non-human studies (Mesulam and Mufson, 1982a,b,c), more recent studies in humans provide strong homology between insular organization (i.e. cytoarchitectonic sub-regions) in non-human primates and humans (Bonthuis et al., 2005; Shaw et al., 2008). The design of methods to specifically demarcate these connectivity-based regions will likely enhance the understanding of insular involvement in general function and in clinical disorders.

Williams syndrome (WS) is a genetic condition associated with the deletion of approximately 20 contiguous genes on chromosome 7. Most individuals with WS have general intellectual disability as well as particular cognitive deficits in visual-spatial, mathematical, and problem-solving abilities (Bellugi et al., 2000). Individuals with WS also typically display hyperaffiliative behavior, atypical expressive language, and enhanced musical interest. WS individuals also express increased incidence of specific phobias, anxiety disorders consisting of an extreme fear of a specific object or situation that is disproportionate to the actual danger or threat. Previous functional imaging studies have shown insular involvement in emotional processing (Damasio et al., 2000; Craig, 2003; Mayer et al., 2006; Rauch et al., 1995; Winkielman et al., 2006; Carr et al., 2003; Phillips et al., 2004) and speech-motor functions (Braun et al., 1997; Corefield et al., 1999; Dronkers, 1996; Price, 2000; Fox et al., 2001; Brown et al., 2005). The insula is involved in reactions to aversive stimuli and representation of aversive experiences (Paulus and Stein, 2006), both physical (i.e. visceral and somatic pain) and emotional (i.e. affect and mood) (Damasio et al., 2000; Zald and Pardo, 2002; Mayer et al., 2006). In particular, the right anterior insula has been identified as a key region of interest in specific phobias (Wright et al., 2003; Paulus and Stein, 2006). While Wright and colleagues examined small animal specific phobia, it is reasonable to assume that insular activity is generalizable to most, if not all, types of specific phobias.

It was hypothesized that the anatomy of insular cortex would be atypical in individuals with WS as compared to healthy matched controls based on their characteristic anomalous social-emotional processing, and exacerbation of specific phobias especially. Atypical anatomy can be defined by atypical size of the region-of-interest (ROI) in the left and/or right cerebral hemisphere, or atypical asymmetry patterns. Examples of atypical ROI volume and asymmetry have been found in other clinical populations. Atypical brain region volume may represent a change in morphology specific to a clinical population (Foundas et al., 2003), while atypical asymmetry could be related to specific behavioral attributes (Foundas et al., 2004), such as stuttering severity. Given the predominant right hemispheric deficits in WS (i.e. emotional anomalies) (Meyer-Lindenberg et al., 2004; Nakamura et al., 2001), it was hypothesized that the WS group would have right hemispheric insular volume reductions. In addition, based on the connectivity of the insular sub-regions and its involvement in specific phobias, it was hypothesized that the anterior sub-region would be more anomalous than the posterior sub-region.

2. Methods

2.1. Insular method reliability

2.1.1. Subjects

Initial reliability was calculated using 3 subjects (6 hemispheres) from Tulane University. All subjects used in this study were right-handed adults. Scans were selected at random from a cohort of neurologically intact adults.

Initial reliability was extended by adding a set of 10 subjects from the Williams syndrome data set that were randomly selected and included in a separate reliability calculation described below.

2.1.2. Data acquisition

Volumetric MR images from Tulane University were acquired for each subject on a GE 1.5 Tesla Signa scanner. T1 weighted images were obtained as a series of 1.5 mm gapless sagittal images. A fast gradient spoil recall was used for the GE scans, with the following parameters: TR = 400, TE = 19, 256 × 256 voxel matrix, 24 cm field of view and 10 degree flip angle. To ensure subject confidentiality and rater blindness, each scan was assigned a subject number. To correct for head position and create a standardized space across images, the MR images were aligned in ANALYZE using the ACPC tool so that the line containing the anterior commissure and posterior commissure, or AC-PC line, was in the horizontal plane.

Coronal brain scans were acquired for each subject from the WS cohort using a GE-Signa 3T scanner (General Electric, Milwaukee, WI) at Stanford University. Coronal brain images were acquired using the following fast 3D volumetric radio frequency spoiled gradient echo pulse sequence parameters: TR = 24 ms, TE = 5 ms, flip angle = 45°, number of excitations = 2, matrix = 256 × 256, field of view = 24 cm, slice thickness = 1.2 mm, 124 contiguous slices.

2.1.3. Image processing

The ANALYZE software package (MAYO Clinic, 1986), version 5.0, was used to process images and determine the volume of the insula and connectivity-based sub-regions in each subject. In order to utilize the program tools, the original scan files for the 3 subjects were stacked using the Import/Export volume tool to create the full brain file in ANALYZE format. All MRI files were aligned along the AC-PC line. Half of the brains were randomly flipped, reversing left and right hemispheres, to insure rater blindness. Within the package, there was a region-of-interest (ROI) function that allowed the rater to create cursor-guided free-hand traces on individual images of desired brain regions. The ROI tracing on each image created an area that was multiplied to slice thickness in order to produce a volume. Region-of-Interest volumes from successive images were then summed to yield a volume, in cubic centimeters, for the full extent of the desired ROI. All summations were calculated within the ANALYZE program.

2.1.4. BrainImageJava

(BIJ) (Ng et al., 2001) (CIBSR.stanford.edu/tools), a freeware program developed in the Center for Interdisciplinary Brain Sciences Research, was used to process images and trace insular ROI volumes in 10 additional subjects. Brain images were stacked, aligned, and skull stripped in BIJ. Insular ROIs were drawn on the spatially aligned images in BIJ, and volumes were determined from the ROI drawings. An insula-specific segmentation tool was built into BIJ that produced the same segmentation capabilities as that used in ANALYZE.

2.1.5. Reliability from ANALYZE and BrainImageJava (BIJ)

Thirteen (13) total brain scans were used to calculate method reliability across two programs, ANALYZE ($N = 3$) and BIJ ($N = 10$).

Measurement reliability was determined by computing an intra-class correlation coefficient (ICC) for the volumes obtained by each rater for each insular region (total, anterior, posterior) and for each hemisphere. Both intra- and inter-rater reliability were obtained. For intra-rater reliability, the insula was measured twice in each hemisphere of the randomly selected brain scans by the first author. Intra-rater reliability was calculated only for total insular volume in ANALYZE ($N = 3$), but included all three ROIs in BIJ ($N = 10$). To determine inter-rater reliability, the insula was measured once in each hemisphere of three (3) brain scans in ANALYZE (by JDC and JRM) and ten (10) different brain scans in BIJ (by JDC and TN). An ICC value greater than or equal to 0.85 was considered reliable.

2.1.6. The insula measure

The insula is a major limbic brain structure that is covered by the frontal, fronto-parietal, and temporal opercula. The opercula form the anterior, superior-lateral and inferior-lateral boundaries of the insula, respectively. The superior and inferior circular sulci separate the insula from the fronto-parietal and temporal opercula, respectively (Fig. 1A). Since the inferior circular sulcus does not extend rostral to the limen of the insula, there is no well-defined boundary between the anterior insula and the orbital frontal cortex. The orbitoinsular sulcus is considered the topographic boundary between the anterior insula and adjacent frontal operculum (orbitofrontal cortex and pars opercularis). The superior and inferior circular sulci fuse to form the posterior pole of the insula, and separate the insula from Heschl's gyrus. The medial boundary of the insula is a band of white matter called the extreme capsule. The orbitoinsular sulcus is viewed best from the sagittal sections,

while the extreme capsule can be visualized most accurately from the coronal view. The circular sulci can be seen from both the sagittal and coronal views, but is most accurately located in the coronal view. That is, the insular ROI mask was drawn first in the sagittal view and refined in the coronal view. Therefore, both the sagittal and coronal sections are utilized in this method.

The insula was first located using the sagittal view. The insula was traced by locating the orbitoinsular, superior and inferior sulci in each sagittal section throughout the full medial to lateral extent (Fig. 1A). Particular attention was paid to the anterior boundary, the orbitoinsular sulcus, in each image; and the posterior boundary, the fusion of the superior and inferior circular sulci. The circular sulci were also traced in the sagittal view, but their greatest accuracy was obtained in the coronal view (Fig. 1C). The current method included traces of all grey matter in sagittal images within these boundaries (Fig. 1A). The medial boundary was set in each coronal image along the anterior-to-posterior extent based upon the location of the extreme capsule (Fig. 1C). Again, the circular sulci, which separate the insula from neighboring opercular cortex, were viewed most accurately from the coronal view, and it is in this orientation where those boundaries were set.

The next step was to divide the insula into sub-regions. The insula can be divided into sub-regions based on either anatomy or connectivity-based compartmentalization. If the insula were divided anatomically, the central sulcus of the insula would be used to separate the insula into anterior and posterior lobules, as was done by Makris et al. (2006). However, this topographic landmark cannot differentiate the connectivity-based sub-regions. The connectivity-based regions of the insula are demarcated by its cytoarchitectonic zones, which each have particular connections with

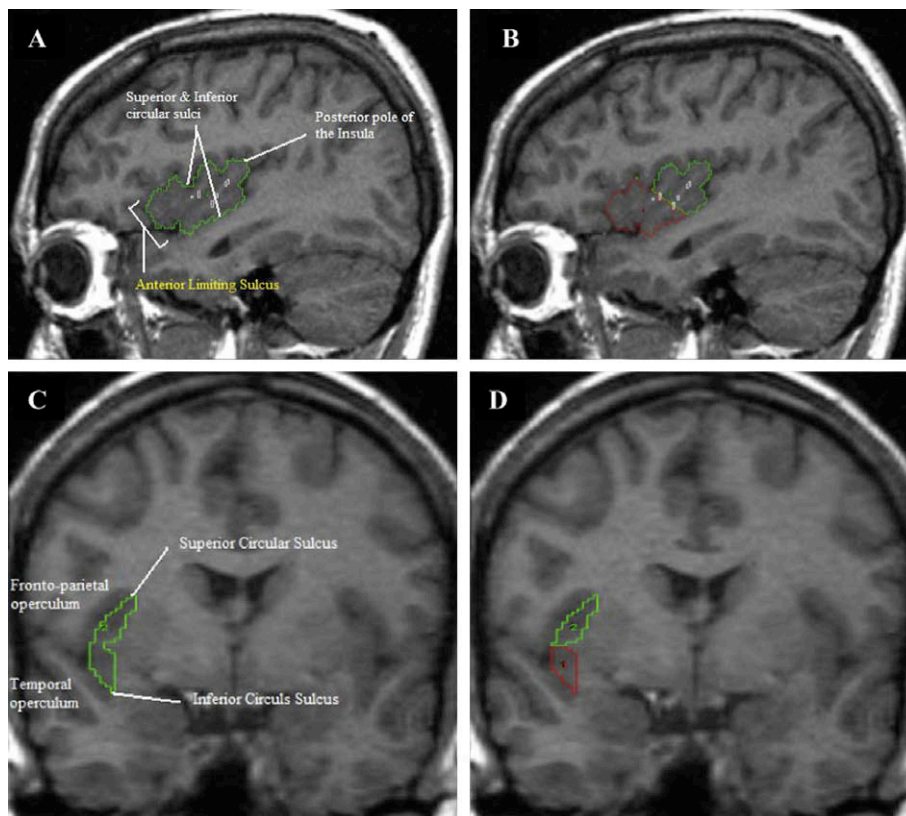


Fig. 1. Insular boundaries. Depicted are the major boundaries used to delineate the insula cortex. The top panels (A and B) show the insula in the sagittal view, which is best for visualizing the anterior limiting sulcus and the posterior pole, but also shows the circular sulci (all labeled in panel A). The bottom panels (C and D) show the insula in the coronal view, which is best for visualizing the circular sulci most accurately and delineating the insula from neighboring opercular cortex (all labeled in panel C). Panels A and C show the total insular ROI, while panels B and D show the insula divided into anterior (red 1) and posterior (green 2). (For interpretation of the references to colour in this figure legend, the reader is referred to the web version of this article.)

other brain regions, and may impart specific functions to specific regions (For review of insular cyto-, myelo-, and chemoarchitectonics and connectivity see Augustine, 1985, 1996). The approximated connectivity-based sub-regions described here are based on the regions outlined by Mesulam and Mufson (1982c), who describe anatomical connections that are predominately distributed in either anteroventral or posterodorsal insula. The anteroventral insula, comprised of the agranular and rostral dysgranular cytoarchitectonic regions, has connections with the parvicellular region of the ventroposteromedial nucleus of the thalamus, primary olfactory cortex, amygdala, hippocampus, anterior cingulate, hypothalamus, periaqueductal gray, orbitofrontal cortex, temporopolar cortex and Brodmann area (BA) 6 (Mesulam and Mufson, 1982b,c). The granular and caudal dysgranular cytoarchitectonic regions, which make up the posterodorsal insula, have connections with distinct brain regions including medial and inferior parietal cortex, primary and secondary somatosensory cortex, primary and secondary auditory cortex, BA 5, supplementary motor area, and contralateral insula. It is important to note, however, that there is no sharp segregation between these regions, and the transition, both cytoarchitectonically and in terms of connectivity, from anteroventral to posterodorsal is gradual (Mesulam and Mufson, 1982a,b; Chikama et al., 1997).

The aim here was to approximate the cytoarchitectonic zones yielding two distinct connectivity-based sub-regions. Approximation of these sub-regions was performed using geometrically-derived boundaries. The most anterior, posterior, inferior, and superior points of the insular ROI were located and used to create the four sides of a rectangular bounding box. A diagonal line based on the central hypotenuse of the rectangle from the anterior–superior corner to inferior–posterior corner divided the insula into anteroventral and posterodorsal and approximated the connectivity-based sub-regions described by Mesulam and Mufson (1982c) (Fig. 2). The result from this geometric division was the angle of the line that divides the insula into anteroventral and posterodorsal functional sub-regions (Fig. 1B and D). It is important to note that the correct angle of the dividing line is set by the bounding rectangle, and the method for approximating that line may be specific to the particular program being used. In ANALYZE, the radial divider tool was used to accomplish this division. An inverse tangent was used to calculate the dividing angle using the height

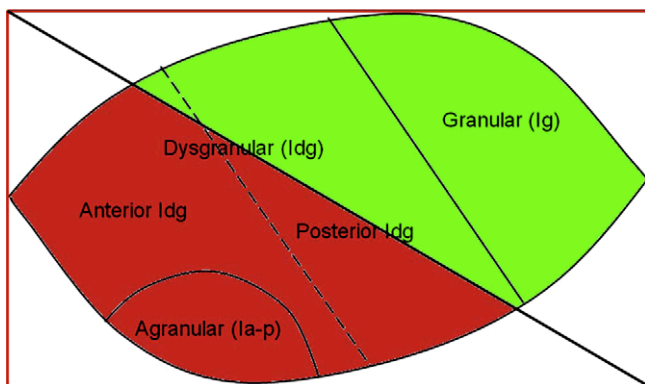


Fig. 2. Rationale for connectivity-based sub-regions. This figure recreates insular topography set forth by Mesulam and Mufson (1982a,b,c), and schematically depicts the rationale and methodology used in the creation of the connectivity-based sub-regions. The red rectangle represents the most anterior, posterior, inferior, and superior points of the insula tracing. The solid diagonal black line across the rectangle is the approximation of the Mesulam's and Mufson sub-regions, and separates the insula into anteroventral (red) and posterodorsal (green). The cytoarchitectonic regions are also marked: Ia-p, agranular-periallocortical; Idg, dysgranular; Ig, granular. (For interpretation of the references to colour in this figure legend, the reader is referred to the web version of this article.)

and length of the bounding box. The resulting angle was set as the starting angle and the number of divisions was set to 2. In BJI, an algorithm tool was implemented to perform these steps automatically.

2.2. Insular morphometry in WS

2.2.1. Subjects

Eleven adults with WS (8 females, 3 males; mean age 27.17 +/- 11.53 years) and 11 healthy age-matched controls (6 females, 5 males; mean age 27.10 +/- 6.75 years) were matched for age and included in the present study (see Table 1). These participants were recruited from the Salk Institute, and genetic diagnosis of WS was established using fluorescent in situ hybridization probes for elastin. All participants gave informed consent to be included in the current study and were native English speakers. All experimental procedures were in compliance with the human subjects committees at the Salk Institute and Stanford University School of Medicine.

2.2.2. Data acquisition

Coronal brain scans were acquired for each subject using a GE-Signa 3T scanner (General Electric, Milwaukee, WI) at Stanford University. Coronal brain images were acquired using the following fast 3D volumetric radio frequency spoiled gradient echo pulse sequence parameters: TR = 24 ms, TE = 5 ms, flip angle = 45°, number of excitations = 2, matrix = 256 x 256, field of view = 24 cm, slice thickness = 1.2 mm, 124 contiguous slices.

2.2.3. Image processing

BJI was used to process images and trace insular ROI volumes. The procedure performed here was the same as that described for BJI in image processing under insular method reliability above.

2.2.4. WS statistics

2.2.4.1. Total brain volume. Total brain volume was calculated using BJI and FMRIB Software Library (FSL) 4.0. The FMRIB Automated Segmentation Tool (FAST) was used to segment and bias correct the images. Total white matter, grey matter, and CSF were computed from the FAST products; total brain volume was computed as the sum of total white matter and total grey matter. A one-way analysis of variance (ANOVA), in which group (WS, control) was the independent variable and total brain volume (in cm³) was the dependent variable, was used to test for group differences in total brain volume.

2.2.4.2. Insular ROIs. A one-way repeated measures analysis of covariance (ANCOVA) was run with hemisphere (left, right) as the repeated measure, group as the independent variable and total insular volume as the dependent variable. In order to control for group differences in total brain volume, total brain volume was entered as a covariate. To test anterior and posterior insular differences, a repeated measures multivariate analysis of covariance

Table 1
Subject demographics.

Group	Gender	Total	Age mean (standard deviations)	Full scale IQ
Controls	Female	6	28.56 (5.10)	117.6 (14.20)
	Male	5	25.91 (8.62)	
	Total	11	27.10 (6.75)	
WS	Female	8	27.64 (13.40)	61.11 (13.24)
	Male	3	25.91 (5.72)	
	Total	11	27.17 (11.53)	

The table above lists the mean (standard deviations) age for each group by gender. Full scale IQ mean (standard deviations) for the total groups is included.

(MANCOVA) was used in which hemisphere was the repeated measure, group was the independent variable, anterior and posterior volumes were the dependent variables, and total brain volume was the covariate.

2.2.4.3. Asymmetry. Asymmetry for each ROI was examined by assessing the group by hemisphere (left, right) interaction that was used in the repeated measures ANCOVA and MANCOVA analyses described above.

3. Results

3.1. Reliability

The reliability of the insular measure method was determined by intra-class correlation coefficient (ICC), and met our *a priori* standards (see Table 2). Intra-rater reliability for the left and right total insula volumes were 0.87 and 0.91, respectively, in ANALYZE. While only total insular volume was used for intra-rater reliability in ANALYZE ($N = 3$), inter-rater ICC was calculated for all insular ROIs in ANALYZE. In ANALYZE ($N = 3$), inter-rater ICC values were all greater than 0.88 (Table 2). For added confidence, intra- (Fig. 3) and inter-rater (Fig. 4) reliability was extended to include an additional 10 MRI scans in BIJ ($N = 10$). Inter-rater reliability using BIJ ($N = 10$) was also good (ICC's > 0.93) (Table 2). Therefore, reliability ICC results were good across imaging programs, ANALYZE and BIJ.

3.2. Williams syndrome

After establishing the reliable morphometry method to quantify insular volume, the method was applied to a sample of WS and matched controls. Due to insular involvement in specific phobias, and the high incidence of specific phobias in WS, atypical insular morphometry was expected in WS. A one-way ANOVA showed no group difference in age ($p = .987$) (Table 2). A one-way ANOVA yielded a significant difference in total brain volume between WS participants and controls ($p = .0002$), which is in agreement with previous findings of total brain volume reduction in WS (Reiss et al., 2004; Chiang et al., 2007). Because of this difference, total brain volume was included as a covariate for all insular volume comparisons. A repeated measures ANCOVA showed a significant difference in total insular volume across groups ($p = .0005$) that was unrelated to hemisphere (Fig. 5A). A repeated measure MANCOVA yielded a significant effect of group at the multivariate level ($p < .001$). Even after accounting for the reduced total brain volumes in WS, the anterior ($p = .002$) (Fig. 5B) and posterior ($p = .0002$) (Fig. 5C) insular volumes were significantly smaller in WS participants compared to controls at the univariate level. Means (in cm^3) and standard deviations for the ROIs are summa-

rized by group in Table 3. Since no normative data on the insula has been reported previously to the author's knowledge, the factor of region (anterior, posterior) was analyzed in the healthy controls to characterize the relationship between anterior and posterior volumes. The anterior region was significantly larger than the posterior region ($p < .001$) and was not related to hemisphere. To be sure, there was no group difference in region.

No significant effect of hemisphere or hemisphere by group interaction was observed for any insular ROI. This result indicates there was no significant asymmetry of anterior, posterior, or total insular volume across hemispheres and no group difference in asymmetry. Again, asymmetry of the healthy controls was examined in greater detail. Asymmetry quotient (AQ) was computed as $(\text{left} - \text{right}) / [(\text{left} + \text{right}) / 2]$ (positive AQ = leftward asymmetry). Controls had rightward asymmetry for anterior (AQ = -0.225), posterior (AQ = -0.039) and total (AQ = -0.0145) insular regions.

4. Discussion

The two main objectives of this study were to develop a reliable method for obtaining volumetric measurements of the human insula, and to validate that method by examining the anatomy of insular cortex in adults with WS and a group of healthy age-matched controls. One advantage of the method reported here is that it utilizes native-space morphometry, which means warping procedures necessary for semi-automated methods (i.e. VBM, etc.) were not used and changes in other gross anatomical features outside the insula, such as gyrfication or brain shape, do not affect insular volume quantification. While the current method quantifies approximated connectivity-based sub-regions of the insula described by Mesulam and Mufson (1982a,b,c), the method reported here is limited in that it does not quantify the distinct insular cytoarchitectonic sub-regions themselves. While the cytoarchitectonic sub-regions of the insula may impart the greatest functional specialization within the insula, these regions are not visible by current MRI technology. However, another advantage of the current method is that it represents the first step in visualizing the insula on the sub-regional level. Statistical reliability was obtained among three raters for this method, supporting its reproducibility not only across raters, but within different software packages. The method described here is potentially transportable to multiple software packages and computer environments as both ANALYZE and BIJ are cross platform compatible. Furthermore, this method includes a procedure for approximating the underlying connectivity-based sub-regions of the insula. This is important as insular connectivity is topographically organized (Mesulam and Mufson, 1982a,b,c), and these connections may impart an organization of insular function as well. This method, or similar methods with the same objective, may allow for more precise examination of structure-function relationships in future studies of insular anatomy in a variety of clinical populations that have previously shown insular volume reduction using other methods (AD, PTSD, schizophrenia) or atypical function of insular cortex (stroke with dysphagia, stuttering, addiction).

The major result of this study was a reduction in both right and left insular volume in the WS group compared to the healthy age-matched controls. It was hypothesized that insular volume reduction would be restricted to the right hemisphere, but proved to be bilateral. When the insula was divided into anterior and posterior sub-regions, both sub-regions were found to be significantly smaller in WS than controls. As opposed to our hypothesis of greater anterior volume reduction, insular volume reduction in WS was diffuse rather than being more pronounced in one sub-region or in one hemisphere. It is also important to note that insular volume reductions in WS were maintained after controlling for total brain

Table 2
Intra-class correlation coefficients by program and region.

Hemisphere	Region	Intra-rater		Inter-rater	
		ANALYZE	BIJ	ANALYZE	BIJ
Left	Anterior	–	0.98	0.96	0.96
	Posterior	–	0.97	0.93	0.97
	Total	0.87	0.98	0.96	0.97
Right	Anterior	–	0.98	0.93	0.93
	Posterior	–	0.98	0.88	0.99
	Total	0.91	0.98	0.92	0.98

The table above lists ICC values for each insular ROI collected in each imaging software package, ANALYZE ($N = 3$) and BIJ ($N = 10$). Intra-rater ICC values were collected by the first author, while inter-rater ICC values were collected by the first three authors.

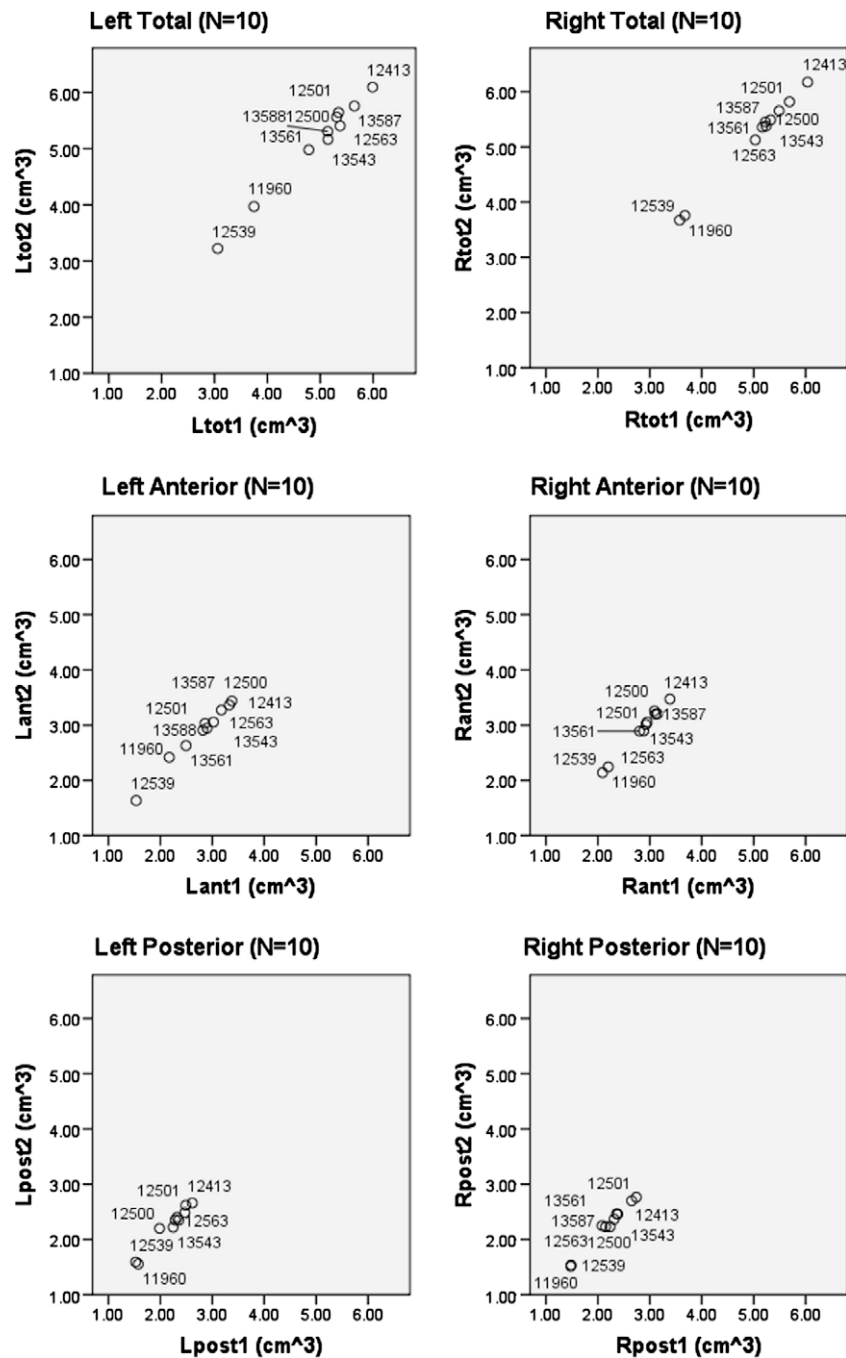


Fig. 3. Scatterplots of intra-rater reliability. The graphs depict measurement 1 and 2 made by the first author for each insular ROI. The left column shows the left hemisphere and the right hemisphere is in the right column. Insular ROIs are organized as total, anterior, and posterior from top to bottom. Measurement 1 is on the x-axis and measurement 2 is on the y-axis. All measurements are in cm³.

volume. Reiss and colleagues (2004) showed changes in insular VBM; however, these results were mixed with one insular peak larger in controls than WS and another larger in WS than controls. There have been reports of other structural anomalies in WS, such as discrete cortical folding abnormalities, differences in gyrification index (Van Essen et al., 2006), and cortical grey matter differences identified with voxel-based morphometry (Boddaert et al., 2006). Cortical thickness has also been found to be increased in the right perisylvian cortex in individuals with WS (Thompson et al., 2005). However, major brain shape differences in WS combined with varied automated methodologies have been suggested by Eckert et al. (2006) to increase the likelihood of spurious neuroanatomical findings in conditions such as WS (2006). This suggests that automated

methodologies are not ideal for quantifying volumetric changes in insular morphometry. In the interest of normative data of the insula and its sub-regions, the healthy controls were found to have rightward AQ for each insular ROI and the anterior insula was consistently larger than the posterior.

There is evidence linking the insula to a wide variety of functional roles. In particular, the insula appears to be important for the representation of aversive experiences, especially fear and anxiety (Paulus and Stein, 2006). WS has a unique relationship with anxiety disorders. While hyperaffiliative behavior is a hallmark of the syndrome, so is an exacerbation of other specific phobias (unrelated to social behavior). The insula has been identified as a key region of interest in specific phobias (Wright et al., 2003),

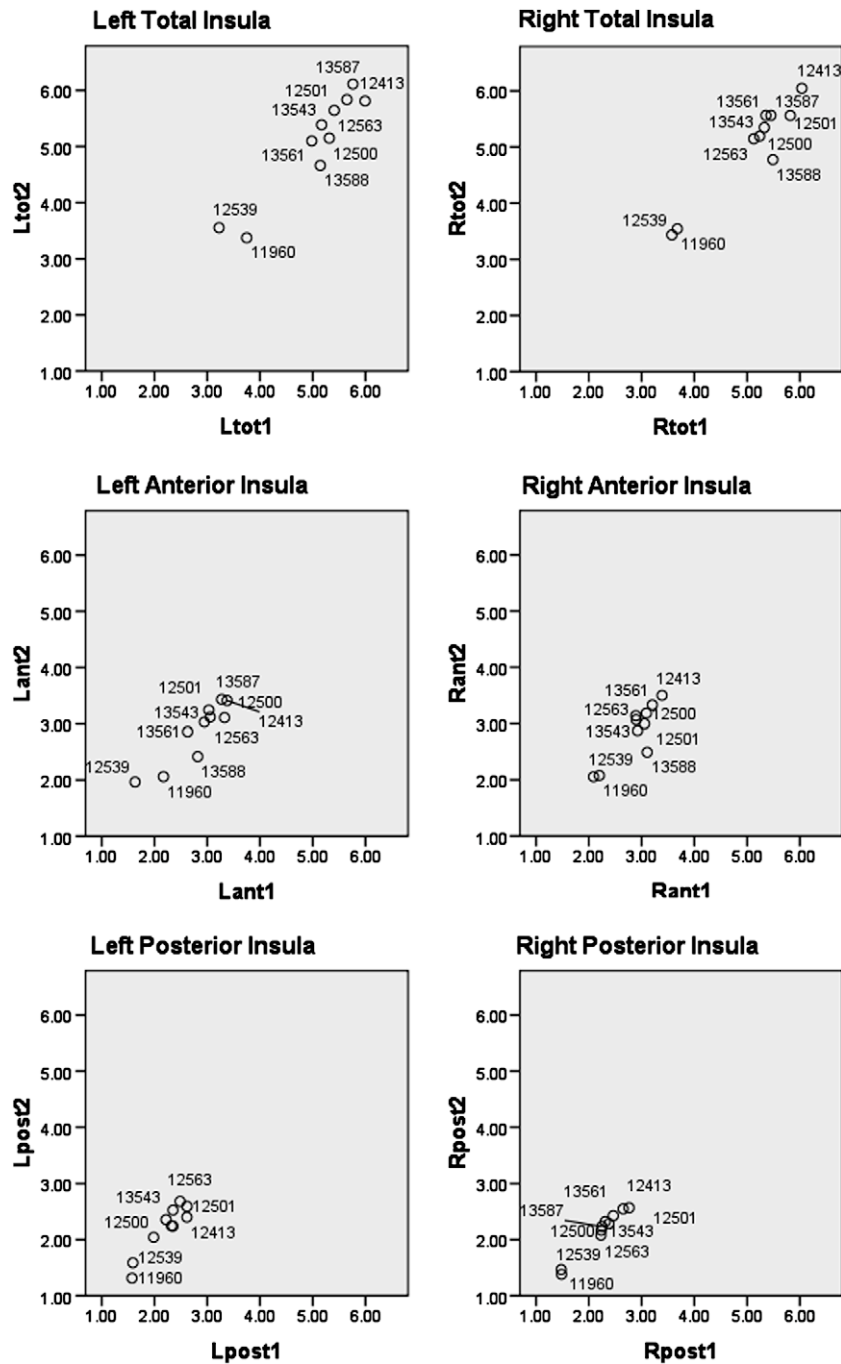


Fig. 4. Scatterplot graphs of reliability measurements by rater 1 and rater 2 using BIJ. The left column shows the left hemisphere and the right hemisphere is in the right column. Insular ROIs are organized as total, anterior, and posterior from top to bottom. Rater 1 is on the x-axis and rater 2 is on the y-axis with all measurements displayed in cm³.

while social phobia is driven more by amygdalar function (Canistraro and Rauch, 2003). A recent functional MRI study of healthy adults probed the sociality of emotional content and found that the insula responded to non-social-emotional stimuli while the amygdala was more responsive to social stimuli (Britton et al., 2005). The amygdala has strong topographic, reciprocal connections with both the anterior and posterior insula (Mufson et al., 1981). Enlarged amygdalar volumes have been reported previously in WS (Reiss et al., 2004), while this study reports diffuse insular volume reduction. Combining present data with previous structural and functional imaging data suggests there may be a functional imbalance between the amygdala and insula

in individuals with WS. This functional imbalance may be related in part to the aberrant anatomy of insular cortex in WS. This imbalance may contribute to a behavioral propensity for greater social affiliation and increased frequency of specific phobias simultaneously. Although speculative, the reduced insular volume in WS may represent a neural risk for the development of hyper-affiliative social behavior with specific phobias, and implicates insular cortex as a critical limbic integrative region as has been proposed by others (Crespo-Facorro et al., 2000; Mesulam and Mufson, 1982c). Future studies should be designed to more directly examine some of these proposed structure–function relationships.

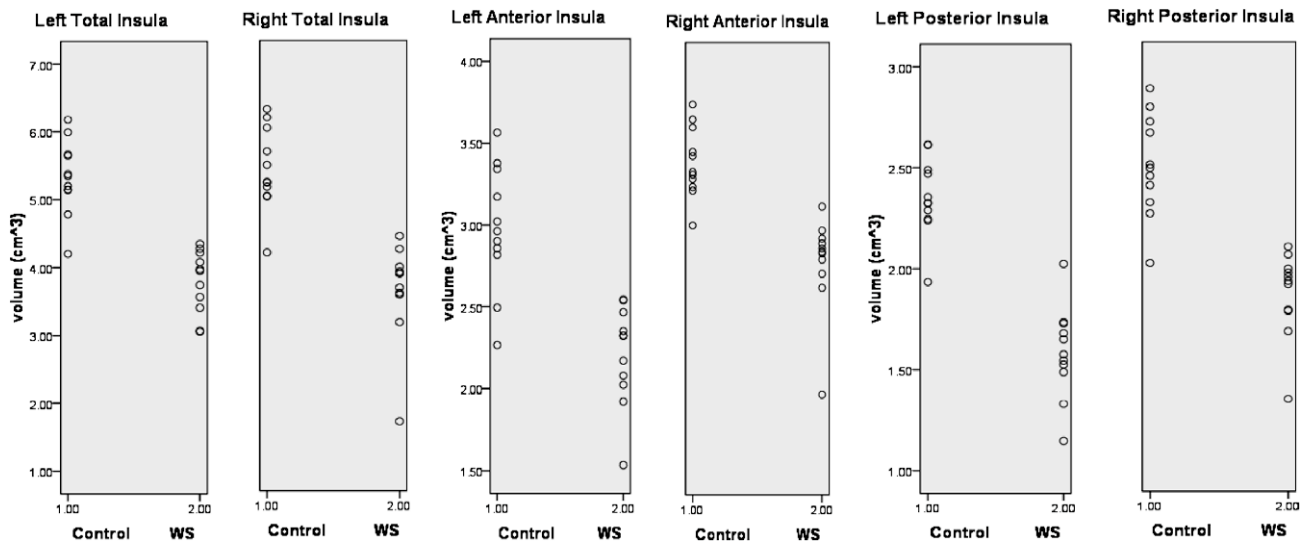


Fig. 5. Insular Raw Volume Scatter Plots. Insular volumes plotted by group and hemisphere for (5A) total insula, (5B) anterior insula, and (5C) posterior insula for each subject in cm^3 .

Table 3
Total brain and insular ROI volumes by group.

Region		Groups	
Hemisphere	ROI	Controls	Williams
Left	Anterior	2.98 (0.38)	2.21 (0.30)
	Posterior	2.35 (0.19)	1.59 (0.23)
	Total	5.33 (0.55)	3.79 (0.46)
Right	Anterior	3.04 (0.35)	2.06 (0.48)
	Posterior	2.38 (0.332)	1.58 (0.27)
	Total	5.442 (0.62)	3.64 (0.73)
Total brain volume		1316.83 (87.41)	1136.41 (94.56)

This table lists means (standard deviations) in cm^3 for total brain volumes and each insular ROI across groups. Individual subject volumes for insular ROIs can be seen in scatter plots in figure 7.

This method brings new focus upon the insula in structural MRI studies related to anxiety, emotional processing and social behavior. It establishes a native-space methodology for measuring the insula as well as segmenting the structure into approximated connectivity-based anterior and posterior regions. Previous studies that examined morphometric differences in insular cortex were limited by either indirect measurements (Foundas et al., 1996, 1997), or automated methods that required brain-warping (Karas et al., 2003, 2004). Furthermore, none of these studies examined connectivity-based sub-regions of the insula. Measuring these sub-regions is important for understanding how the insula may play a role in specific symptoms of clinical disorders. This method will allow researchers to probe insular morphology more precisely in clinical populations, particularly those related to anxiety and aberrant social behavior. It will also allow for further exploration and establishment of asymmetry patterns in healthy control populations and potential deviations in clinical populations. New algorithm development that allows for fully automated and accurate segmentation of the insula will allow for this work to proceed more efficiently and rapidly in the future.

Conflict of interests

I, Jeremy Cohen, have no conflicts of interest. I have no financial ties to any people or organizations that could have influenced this research study.

Contributors

Jeremy Cohen: author, data collector, data analysis.
 Jeffrey R. Mock: ANALYZE reliability rater.
 Taylor Nichols: BIJ reliability rater.
 Janet Zalina: data collection from Tulane University.
 David M. Corey: Thesis committee member who contributed to the method development used in this paper.
 Lisa Lemen: MR physicist for Tulane University and assisted with data collection.
 Ursula Bellugi: Salk Institute collaborator for WS subject recruitment.
 Albert Galaburda: contributor to Yale, NIH 5 R01 NS027116.
 Allan L. Reiss: T32 adviser, contributor to Yale, NIH 5 R01 NS027116.
 Anne L. Foundas: Thesis adviser and contributed to the method development used in this paper.

Role of funding sources

This work was supported by NIH (Foundas, DCO4957), (T32, NIH 5 T32 MH019908), (Yale, NIH 5 R01 NS027116), Louisiana Board of Regents and the General Clinical Research Centers (GCRC), VA Merit Review Grant (Foundas), and NICHD (P01 HD033113–12). The NIH, GCRC, VA, and NICHD had no further role in the study design; collection, analysis, and interpretation of data; writing of the report; and decision to submit the paper for publication.

Acknowledgements

The author would like to thank Dr. Murray Ettinger, who assisted with advice and proof-reading of the manuscript.

References

- Augustine JR. The insular lobe in primates including humans. *Neurology Research* 1985;7:2–10.
- Augustine JR. Circuitry and functional aspects of the insular lobe in primates including humans. *Brain Research Review* 1996;22:229–44.
- Bellugi U, Lichtenberger L, Jones W, Lai Z, St George MI. The cognitive profile of Williams syndrome: a complex pattern of strengths and weaknesses. *Journal of Cognitive Neuroscience* 2000;12(Suppl 1):7–29.

- Boddaert N, Mochel F, Meresse I, Seidenwurm D, Cachia A, Brunelle F, et al. Parieto-occipital grey matter abnormalities in children with Williams syndrome. *NeuroImage* 2006;30:721–5.
- Bonthuis DJ, Solodkin A, Van Hoesen GW. Pathology of the insular cortex in Alzheimer disease depends on cortical architecture. *Journal of Neuropathology & Experimental Neurology* 2005;64:910–22.
- Braun AR, Varga M, Stager S, Schulz G, Selbie S, Maisog JM, et al. Altered patterns of cerebral activity during speech and language production in developmental stuttering: an H₂O¹⁵ positron emission tomography study. *Brain* 1997;120:761–84.
- Britton JC, Phan KL, Taylor SF, Welsh RC, Berridge KC, Liberzon I. Neural correlates of social and nonsocial emotions: an fMRI study. *NeuroImage* 2005;31:397–409.
- Brown S, Ingham RJ, Ingham JC, Laird AR, Fox PT. Stuttered and fluent speech production: an ALE meta-analysis of neuroimaging studies. *Human Brain Mapping* 2005;25:105–17.
- Cannistraro PA, Rauch SL. Neural circuitry of anxiety: evidence from structural and functional neuroimaging studies. *Brain Imaging* 2003;37(4):8–25.
- Carr L, Iacoboni M, Dubeau M-C, Mazziotti JC, Lenzi GL. Neural mechanisms of empathy in humans: a relay from neural systems for imitation to limbic areas. *Neuroscience* 2003;100(9):5497–502.
- Chiang MC, Reiss AL, Lee AD, Bellugi U, Galaburda AM, Korenberg JR, et al. 3D pattern of brain abnormalities in Williams syndrome visualized using tensor-based morphometry. *NeuroImage* 2007;36:1096–9.
- Chikama M, McFarland NR, Amaral DG, Haber SN. Insular cortical projections to functional regions of the striatum correlate with cortical cytoarchitectonics organization in the primate. *Journal of Neuroscience* 1997;17(24):9686–705.
- Corefield DR, Murphy K, Josephs O, Fink GR, Frackowiak RSJ, Guz A, et al. Cortical and subcortical control of tongue movement in humans: a functional neuroimaging study using fMRI. *Journal of Applied Physiology* 1999;86(5):1468–77.
- Craig AD. Interoception: the sense of the physiological condition of the body. *Current Opinion in Neurobiology* 2003;13:500–5.
- Crespo-Facorro B, Kim J-J, Andreasen NC, O'Leary DS, Bockholt HJ, Magnotta V. Insular cortex abnormalities in schizophrenia: a structural magnetic resonance imaging study of first-episode patients. *Schizophrenia Research* 2000;46:35–43.
- Damasio AR, Grabowski TJ, Bechara A, Damasio H, Ponto LL, Parvizi J, et al. Subcortical and cortical brain activity during the feeling of self-generated emotions. *Nature Neuroscience* 2000;3(10):1049–56.
- Desikan RS, Segonne F, Fischl B, Quinn BT, Dickerson BC, Blacker D, et al. An automated labeling system for subdividing the human cerebral cortex on MRI scans into gyral based regions of interest. *NeuroImage* 2006;31(3):968–80.
- Dronkers NF. A new brain region for coordinating speech articulation. *Nature* 1996;384:159–61.
- Eckert MA, Tenforde A, Galaburda AM, Bellugi U, Korenberg JR, Mills D, et al. To modulate or not to modulate: differing results in uniquely shaped Williams syndrome brains. *NeuroImage* 2006;32(3):1001–7.
- Foundas AL, Eure KF, Seltzer B. Conventional MRI volumetric measures of parietal and insular cortex in Alzheimer's disease. *Progress in Neuropsychopharmacology and Biological Psychiatry* 1996;20:1131–44.
- Foundas AL, Leonard CM, Mahoney SM, Agee OF, Heilman KM. Atrophy of the hippocampus, parietal cortex, and insula in Alzheimer's disease: a volumetric magnetic resonance imaging study. *Neuropsychiatry, Neuropsychology and Behavioral Neurology* 1997;10(2):81–9.
- Foundas AL, Corey DM, Angeles V, Bollich AM, Crabtree-Hartman E, Heilman KM. A typical cerebral laterality in adults with persistent developmental stuttering. *Neurology* 2003;61:1378–85.
- Foundas AL, Bollich AM, Feldman J, Corey DM, Hurley M, Lemen LC, et al. Aberrant auditory processing and atypical planum temporale in developmental stuttering. *Neurology* 2004;63:1640–6.
- Fox PT, Huang A, Parsons LM, Xiong J-H, Zamariipa F, Rainey L, et al. Location-probability profiles of the mouth region of human primary motor-sensory cortex: model and validation. *NeuroImage* 2001;13:196–209.
- Karas GB, Burton EJ, Rombouts SARb, van Schijndel RA, O'Brien JT, Sheltens P, McKeith IG, Williams D, Ballard C, Barkhof F. A comprehensive study of gray matter loss in patients with Alzheimer's disease using optimized voxel-based morphometry. *NeuroImage* 2003;18:895–907.
- Karas GB, Sheltens P, Rombouts SARb, Visser PJ, van Schijndel RA, Fox NC, et al. Global and local gray matter loss in mild cognitive impairment and Alzheimer's disease. *NeuroImage* 2004;23:708–16.
- Makris N, Goldstein JM, Kennedy D, Hodge SM, Caviness VS, Faraone SV, et al. Decreased volume of left and total anterior insular lobule in schizophrenia. *Schizophrenia Research* 2006;83:155–71.
- Mayer EA, Naliboff BD, Craig AD. Neuroimaging of the brain-gut axis: from basic understanding to treatment of functional GI disorders. *Gastroenterology* 2006;131:1925–42.
- Mechelli A, Price CJ, Friston KJ, Ashburner J. Voxel-based morphometry of the human brain: methods and applications. *Current Medical Imaging Reviews* 2005;1(1):1–9.
- Mesulam M-M, Mufson EJ. Insula of the old world monkey I: architectonics in the insulo-orbito-temporal component of the paralimbic brain. *Journal of Comparative Neurology* 1982a;212:1–22.
- Mesulam M-M, Mufson EJ. Insula of the old world monkey II: afferent cortical input and components of the claustrum. *Journal of Comparative Neurology* 1982b;212:23–37.
- Mesulam M-M, Mufson EJ. Insula of the old world monkey III: efferent cortical output and comments on function. *Journal of Comparative Neurology* 1982c;212:38–52.
- Meyer-Lindenberg A, Kohn P, Mervis C, Kippenhan J, Olsen R, Morris C, et al. Neural basis for genetically determined visuospatial construction deficit in Williams syndrome. *Neuron* 2004;43:623–31.
- Mufson EJ, Mesulam M-M, Pandya DN. Insular interconnections with amygdala in the rhesus monkey. *Neuroscience* 1981;6(7):1231–48.
- Naidich TP, Kang E, Fatterpekar GM, Delman BN, Gultekin SH, Wolfe D, et al. The insula: anatomic study and MR imaging display at 1.5 T. *American Journal of Neuroradiology* 2004;25:222–32.
- Nakamura M, Watanabe K, Matsumoto A, Yamanaka T, Kumagai T, Miyazaki S, et al. Williams syndrome and deficiency in visuospatial recognition. *Developmental Medicine & Child Neurology* 2001;43:617–21.
- Ng YR, Shiffman S, Brosnan TJ, Links JM, Beach LS, Judge NS, et al. BrainImageJ: a Java-based framework for interoperability in neuroscience, with specific application to neuroimaging. *Journal of the American Medical Informatics Association* 2001;8(5):431–42.
- Oppenheimer SM, Gelb A, Girvin JP, Hachinski VC. Cardiovascular effects of human insular cortex stimulation. *Neurology* 1992;42(9):1727–32.
- Paulus MP, Stein MB. An insular view of anxiety. *Biological Psychiatry* 2006;60(4):383–7.
- Phillips ML, Williams LM, Heining M, Herba CM, Russell T, Andrew C, et al. Differential neural responses to overt and covert presentations of facial expressions of fear and disgust. *NeuroImage* 2004;21:1484–96.
- Price CJ. The anatomy of language: contributions from functional neuroimaging. *Journal of Anatomy* 2000;197:335–59.
- Rauch SL, Savage CR, Alpert NM, Miguel EC, Baer L, Breiter HC, et al. A positron emission tomographic study of simple phobic symptom provocation. *Archives of General Psychiatry* 1995;52(1):20–8.
- Reiss AL, Eckert MA, Rose FE, Karchemskiy A, Kesler S, Chang M, et al. An experiment of nature: brain anatomy parallels cognition and behavior in Williams syndrome. *Journal of Neuroscience* 2004;24(21):5009–15.
- Shaw P, Kabani N, Lerch J, Eckstrand K, Lenroot R, Gogtay N, et al. Neurodevelopmental trajectories of the human cerebral cortex. *Journal of Neuroscience* 2008;28:3586–94.
- Thompson PM, Mega MS, Toga AW. Disease specific brain atlases. In: Mazziotta JC et al., editors. *Brain mapping: the disorders*. Academic Press; 2000a.
- Thompson PM, Mega MS, Toga AW. Disease-Specific Probabilistic Brain Atlases. *IEEE Workshop on Mathematical Methods in Biomedical Image Analysis*, South Carolina, 2000b.
- Thompson PM, Lee AD, Dutton RA, Geaga JA, Hayashi KM, Eckert MA, et al. Abnormal cortical complexity and thickness profiles mapped in Williams syndrome. *Journal of Neuroscience* 2005;25(16):4146–58.
- Van Essen DC, Dierker D, Snyder AZ, Raichle ME, Reiss AL, Korenberg J. Symmetry of cortical folding abnormalities in Williams syndrome revealed by surface-based analyses. *Journal of Neuroscience* 2006;26(20):5470–83.
- Winkielman P, Knutson B, Paulus M, Trujillo JL. Affective influence on judgements and decisions: moving towards core mechanisms. *Review of General Psychology* 2007;11:179–92.
- Wright CI, Martis B, McMullin K, Shin LM, Rauch SL. Amygdala and insular responses to emotionally valenced human faces in small animal specific phobia. *Biological Psychiatry* 2003;54:1067–76.
- Yaxley S, Rolls ET, Sienkiewicz ZJ. Gustatory responses of single neurons in the insula of the macaque monkey. *Journal of Neurophysiology* 1990;63(4):689–700.
- Zald DH, Pardo JV. The neural correlates of aversive auditory stimulation. *NeuroImage* 2002;16(3):746–53.